

Chapter 13.

Range and Angle Tracking

13.1. Introduction

Estimation of the position of a moving target is generally referred to as “tracking”. For most time-of-flight sensors that operate in polar space, this process involves following the target independently in both range and angles to obtain good estimates of its position in 3D. This chapter is concerned with the mechanics of this tracking process.

13.2. Range Estimation and Tracking

Range Tracking is an extension to the independent measurement of range on a pulse by pulse or block (integrated) by block basis. It involves using the previous estimate of the range and range rate to predict the where the target will be in time for the next range measurement. The most common configuration uses a type-2 loop (2 cascaded integrators or their equivalent) to give zero lag for constant range-rate targets.

In the radar context, standard estimation techniques were introduced first to automate the process of plot extraction for individual aircraft targets observed by surveillance radars. This is a process called “track while scan” and is discussed in Chapter 15.

13.2.1. Range gating

Range gating process consists of sampling the received video signal at a specified time after the transmit pulse has been radiated. This involves measuring the amplitude of this signal over a short period using some form of electronic switch that charges a capacitor, or a sample-and-hold (S&H) IC which performs a similar function

The sample period should be about equal to the length of the transmitted pulse so that the maximum amount of pulse energy and the minimum amount of noise is incorporated into each sample.

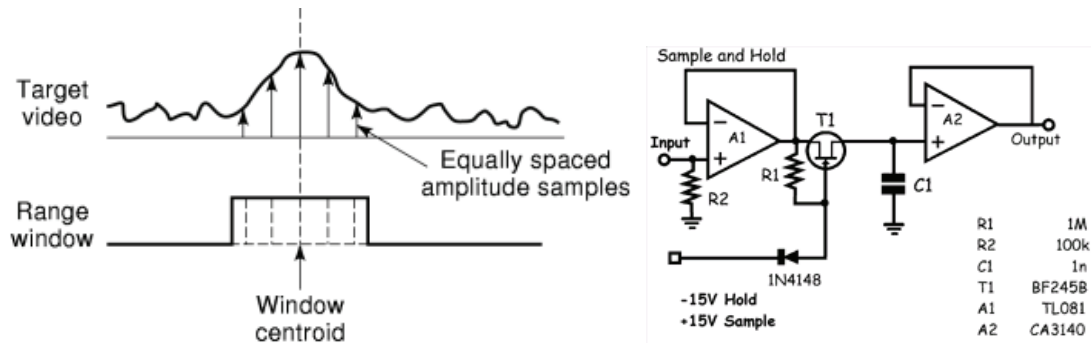


Figure 13.1: Sampling an echo pulse is known as range gating

13.2.2. Principles of a Split-Gate Tracker

A split gate tracker consists of two S&H circuits separated in time (range) by about one pulse width. They are known as the Early and Late gates. In early analog systems, these were in fact FET switches that allowed charge to flow into an integrator for the gate period τ_e and τ_l as shown in the figure below.

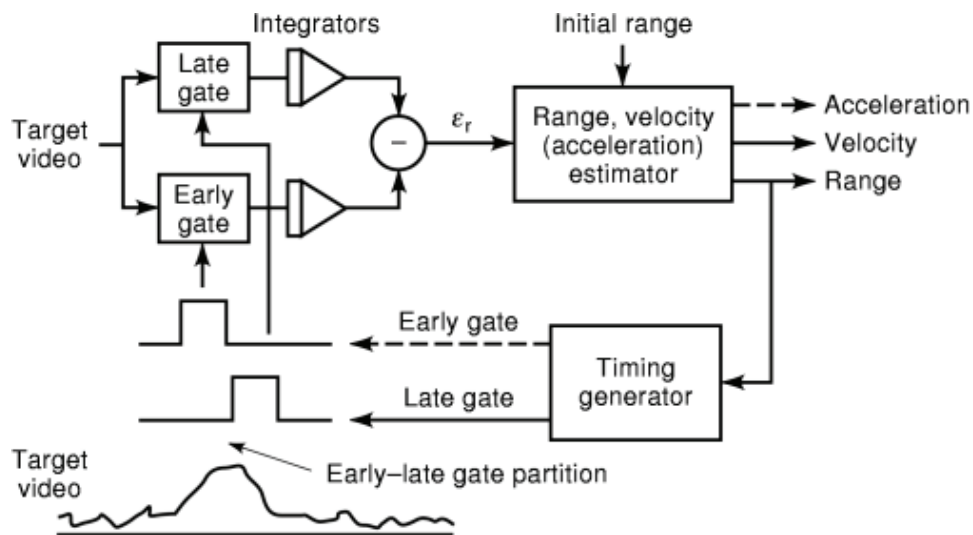


Figure 13.2: Analog split gate tracker

13.2.3. Range Transfer Function

At the time corresponding to the estimated target range, these S&Hs are triggered, one, one half pulsewidth prior to the estimated range delay, and one the same period after. If the range estimate is accurate, they sample equal amplitudes of the target echo pulse on either side of the peak as shown in the diagram, and the difference between the two gate voltages $V_L - V_E = 0$. However, if there is a small range error then the contents of the one gate will be larger than the contents of the other and the difference will not be zero.

To measure the transfer function, it is possible to keep the gates still and move the target through the gates, or visa versa. The following figure shows the measured range transfer function for an ultrasonic radar simulation

Note that the sign and magnitude of the error will drive the tracking error toward zero only over a limited range (in this case, about 20 samples) and the “linear” region over which the magnitude of the range error can be used to estimate the actual error is more limited (about 8 samples).

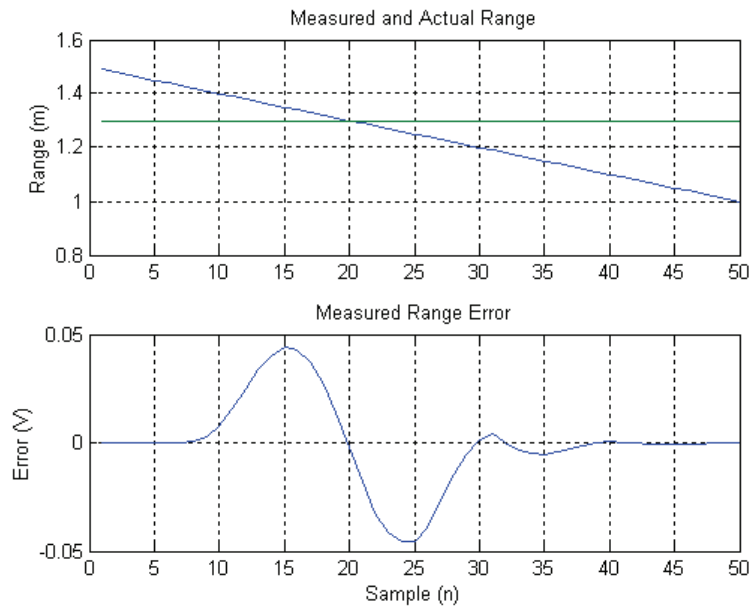


Figure 13.3: Measured transfer function for an ultrasonic range tracker

The range tracking loop uses this error to drive the smoothed estimate of the target range until the amplitudes of the early and late gate samples are equal. If, however, the error falls outside the bounds shown by the transfer function, then the error voltage falls to zero (in a noise free environment) and there is no driving function.

13.2.4. Noise on Split Gate Trackers

According to Barton, the best noise performance is achieved when the matched filter is matched to the pulse spectrum ($1 < B \cdot \tau < 2$) and then the range gate width is matched to the pulse width ($\tau < \tau_g < 2\tau$). This leads to an error slope, $k_r = 2.5$, and a normalised RMS tracking error given by

$$\sigma_r = \frac{\tau}{2.5\sqrt{2S/N}} \quad (13.1)$$

Note that the tracking error will take on the dimensions of τ , so it can be a range error in metres or a delay error in seconds.

13.2.5. Tracking and Estimation

The process applies simple estimation theory to predict where the target will be and by placing the gates at the correct range prior to the measurement taking place it improves the measurement accuracy. Placing the range gates as accurately as possible has two primary functions. In the first instance it ensures that any residual errors are within the linear region of the range transfer function and are close to the true error.

Secondly, by sampling the echo signal close to its peak ensures that the measurement SNR is as high as possible.

Typically a range tracker will include three gates, the early and late gates discussed earlier, and a sum gate which straddles the other two gates and samples the whole received pulse. This gate can be a physical realisation as shown in the figure below, or it can be the sum of the voltage signals from the early and late gates.

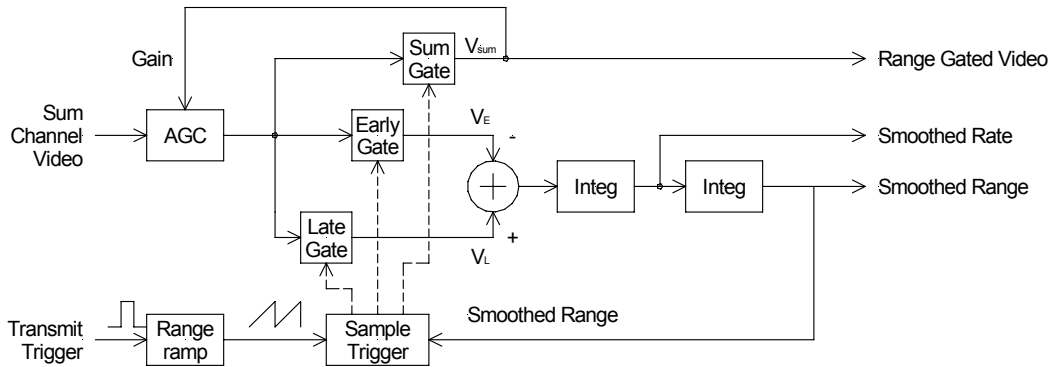


Figure 13.4: Analog tracking loop implementation using cascaded integrators

To maintain a constant loop bandwidth, the error function $V_L - V_E$ must be normalised otherwise targets with a large RCS, or closer to the radar will produce larger errors than one with a small RCS or further away even if the true range error is the same. Normalisation is achieved using an automatic gain control (ACG) driven by the sum channel range gated video signal to maintain a constant target amplitude in the receiver irrespective of the range or the target RCS

The normalised range error drives a second order tracker, represented in the figure by a pair of cascaded integrators. In most modern trackers digital implementations of the tracking loop are used as they are easy to implement and can be optimised to suit specific conditions. Problems with pure digital implementations such as the one shown in the figure below is that the S&H and ADC must have sufficient dynamic range to digitise the full range of target amplitude variations. This can exceed 80dB.

The primary object of such tracking filters is to minimise the output noise variance under specific conditions of input. (usually constant velocity).

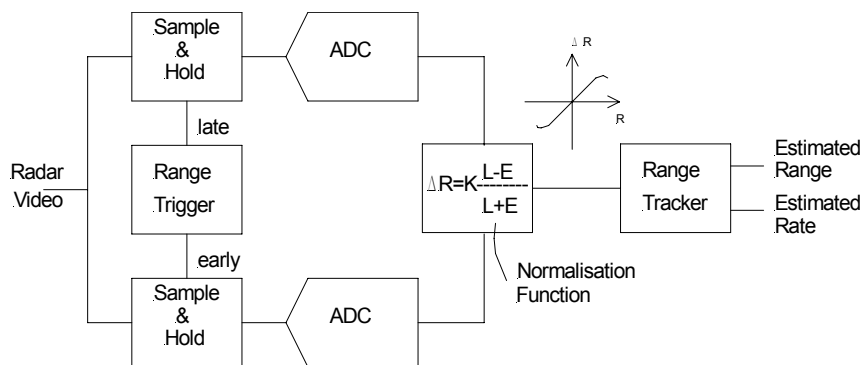


Figure 13.5: Digital tracking loop implementation

Kalman filters and α - β trackers are widely used for track-while-scan and single target tracking applications.

The α - β Filter

The α - β tracker is a fixed gain formulation of the Kalman filter and is still widely used because it is easy to implement performs well in general.

The α - β Tracker equations for range tracking are defined below

Smoothing

$$\hat{R}_n = \hat{R}_{pn} + \alpha(R_n - \hat{R}_{pn}) \quad (13.2)$$

$$\hat{V}_n = \hat{V}_{pn} + \frac{\beta}{T_s}(R_n - \hat{R}_{pn}) \quad (13.3)$$

Prediction

$$\hat{R}_{p(n+1)} = \hat{R}_n + \hat{V}_n T_s \quad (13.4)$$

$$\hat{V}_{p(n+1)} = \hat{V}_n \quad (13.5)$$

where: \hat{R}_n = Smoothed Estimate of Range

\hat{V}_n = Smoothed estimate of Range Rate

R_n = Measured Range

$\hat{R}_{p(n+1)}$ = Predicted range after T seconds

$\hat{V}_{p(n+1)}$ = Predicted Range Rate after T seconds

\hat{R}_{pn} = Predicted range at the Measurement Time

\hat{V}_{pn} = Predicted Velocity at the Measurement Time

T_s = Sample Time

α, β = Smoothing Constants

It has been suggested (Benedict and Bordner) that to minimise the output noise variance at steady state, and the transient response to a manoeuvring target as modelled by a ramp function, then the gain coefficients are related as

$$\beta = \frac{\alpha^2}{2 - \alpha}. \quad (13.6)$$

Other criteria can also be used. For example, it has been suggested that the filter should have the fastest possible step response (critical damping), in which case the coefficients are related as

$$\alpha = 2\sqrt{\beta} - \beta. \quad (13.7)$$

The actual values of the gains depend on the sample period, the predicted target dynamics and the required loop bandwidth.

The main disadvantage of the fixed gain α - β tracker is that it estimates the position of an accelerating target with a constant lag. The magnitude of this lag can easily be estimated and the filter can use adaptive gains to improve the RMS tracking accuracy under these circumstances. The cost function that is minimised is $[lag^2 + \sigma_r^2]$.

For estimates that include accelerations, the α - β - γ tracker can be substituted. However, its performance if the target is moving with constant velocity is poorer than that for the simple α - β tracker because of the additional noise introduced by the acceleration estimate.

The Kalman Filter

A simplified view of the Kalman filter when compared to one of the sub-optimal filters is that it uses optimum weighting coefficients (somewhat analogous to α and β) that are dynamically computed each update cycle. In addition a more precise model of the target dynamics can be used.

The benefits of the additional complexity include

- Improvement in tracking accuracy
- A running measure of the accuracy
- Method of handling measurements of variable accuracy, non uniform sample rate or missing samples
- Higher order systems are easier to handle

13.2.6. Ultrasonic Range Tracker Example

An ultrasonic range tracker based on the matched filter simulation described earlier in these notes has been developed to evaluate the effects of various gate and tracking filter parameters. In the following figure an approaching target is shown starting at a range of 1.5m and moving towards the sensor. The tracking gates are placed at a range of 1m.

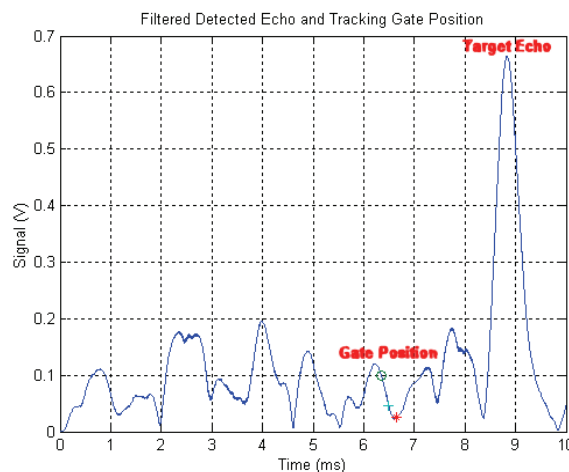


Figure 13.6: The target echo and the split gate position at the start of the simulation

To perform the split gate tracking function, three gates are shown, the early and the late gates straddling the sum (central) gate (o,+,*). Due to receiver noise, the tracking gates will move in a random fashion until they are reached by the target echo, at which time they will lock onto it.

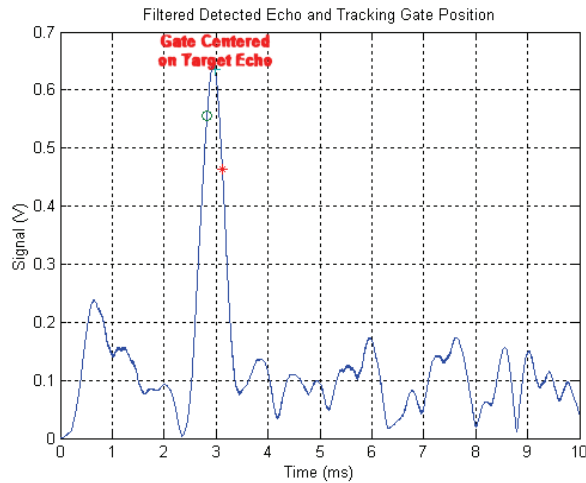


Figure 13.7: Target echo and split gate position during tracking

Note that the early and late gates are sitting astride the target echo peak which would produce a small tracking error voltage that drives the tracking loop to maintain its position straddling the target echo perfectly, even though the latter is moving.

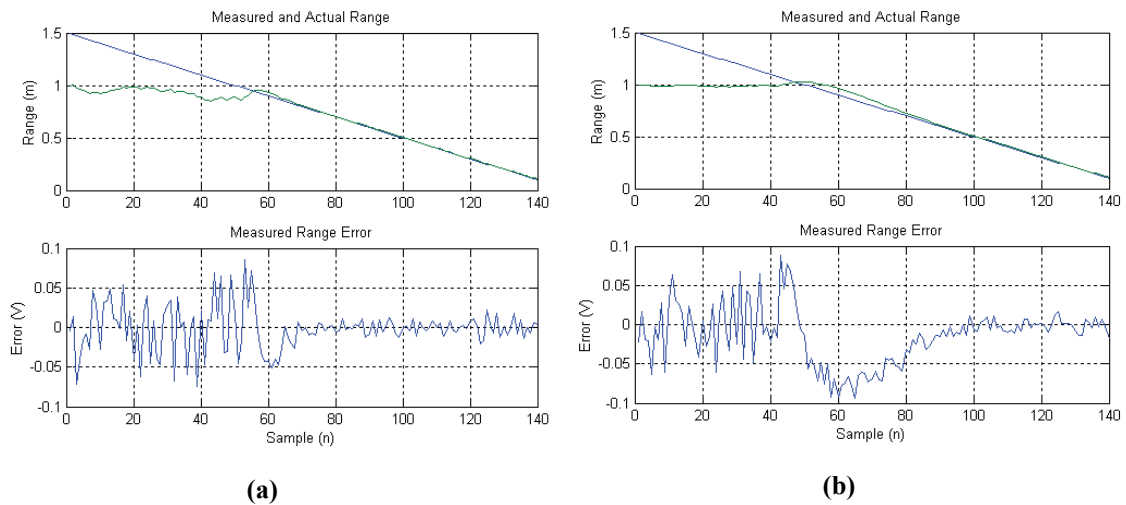


Figure 13.8: Target range, measured range and track error with time for (a) $\alpha = 0.3$ (b) $\alpha = 0.1$

13.2.7. Tracking Noise after Filtering

An α - β filter (with Benedict-Bordner gains) takes the error signal produced by the split gate tracker and produces estimates of the position and the rate. The one-sample-ahead position estimate is fed back into the range gate timing circuitry to trigger the early and late gate samples.

Note that for large α , the measured noise has a larger effect on the gate position than the for small α but that the filter settles onto the target much more quickly once the

two coincide. In general this settling period can be reduced by injecting course estimates of the target rate into the track filter, or by starting out with a filter with a wider bandwidth and progressively reducing it as the tracking error decreases

The tracking noise, being the difference between the measured and the true target position (for constant vel target) is inversely proportional to the filter bandwidth.

The filter performance is often characterised by the ratio in the variances of the output and input noise. This is known as the Variance Reduction Ratio (VRR). Measurements made over n samples combine in the filter to provide an output whose RMS noise is reduced by $1/\sqrt{n}$ compared to a single pulse measurement.

In terms of the equivalent noise bandwidth β_n of the range filter,

$$n = \frac{f_r}{2\beta_n} = \frac{1}{VRR}, \quad (13.8)$$

where VRR – Variance reduction ratio,
 f_r – Pulse repetition frequency (Hz),
 β_n - Bandwidth of tracking filter (Hz).

For the split gate tracker, the filtered thermal noise output will therefore be

$$\sigma_r = \frac{\tau}{2.5\sqrt{(S/N)(f_r/\beta_n)}}. \quad (13.9)$$

The following figure shows the filter transfer function (for the position estimate) for various values of α and β (using the Benedict Bordner relationship).

The filter half power bandwidth is measured at $|H(z)| = 0.707$.

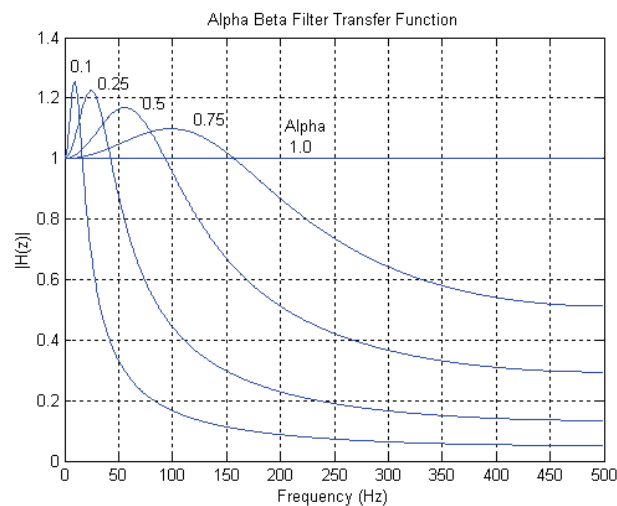


Figure 13.9: The α - β filter transfer function for a sample rate of 1kHz

It can be seen that the filter bandwidth increases as α increases, but that the relationship is not completely linear. As stated earlier in these notes, a filter can be

characterised completely by its impulse response. This allows the VRR to be determined as a ratio of the power in the impulse response to the power in the impulse. This is valid because the frequency spectrum of an impulse is flat whereas the response will be low-passed as shown in the figure. Alternative methods of calculating the VRR is to inject white noise of known variance into the filter and to measure the variance on the output, or by integrating the area under the $|H(z)|^2$ curve in the frequency domain. In general, the impulse response method converges very quickly and so has been used to determine the VRR plotted in the following figure.

Using the VRR formulation, the filtered tracking noise can be rewritten as

$$\sigma_r = \frac{\tau}{2.5\sqrt{2S/N}} \sqrt{VRR}. \quad (13.10)$$

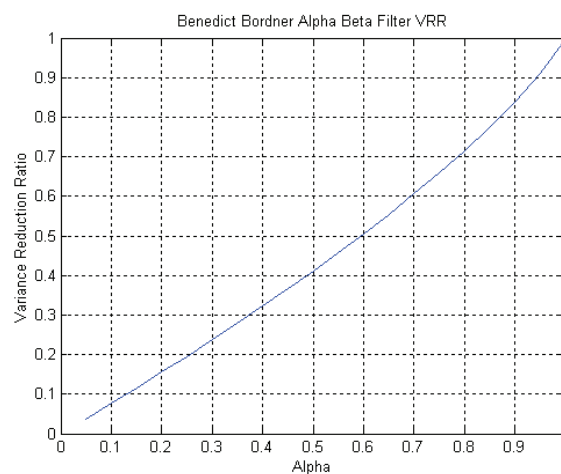


Figure 13.10: The α - β filter variance reduction ratio as a function of α

13.2.8. Tracking Lag for an Accelerating Target

The lag in the position estimate of an accelerating target is a function of the sample time T_s , the gains and the magnitude of the acceleration.

For the α - β filter, the lag as a function of the two gains is

$$L = \ddot{r} \frac{T_s^2}{\beta} (1 - \alpha), \quad (13.11)$$

where L – Lag (m),
 \ddot{r} – Range acceleration (m/s^2),
 T_s – Sample interval (sec),
 $\alpha\beta$ - Filter gains.

For a sample rate of 1kHz ($T_s=1\text{ms}$) and an acceleration of 1m/s^2 , the following figure shows the lag as a function of α for a Benedict Bordner α - β filter. Because of the fast sample rate, this lag is insignificant unless the target acceleration is very high

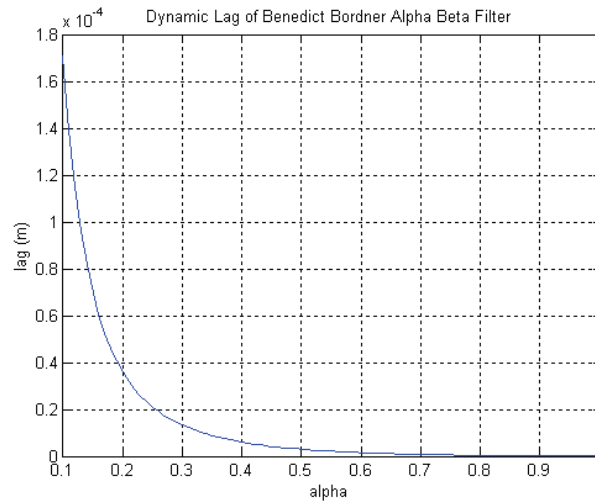


Figure 13.11: The α - β filter dynamic lag for a sample time of 1ms and an acceleration of 1m/s^2 as a function of α

13.2.9. Range Tracker Bandwidth Optimisation Example

As discussed earlier in this chapter, as the tracking filter bandwidth increases, the dynamic lag decreases. To minimise the mean squared tracking error the cost function that is minimised is $[\text{lag}^2 + \sigma_r^2]$. In this example, the α - β tracker must be optimised to track a missile with the following parameters:

- Target acceleration of 1g
- Split gate tracker with a gate size of 3m
- Signal to Noise Ratio assumed to be 10dB (thermal noise only)
- Sample rate 50Hz

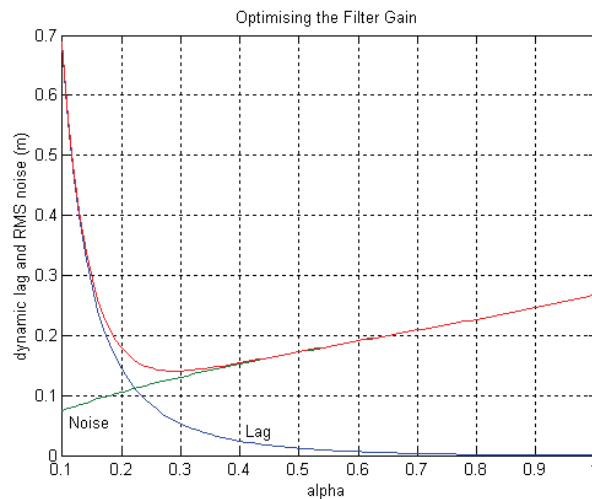


Figure 13.12: RMS noise and dynamic lag and the root mean squared sum determines the optimum gain

Using the equations developed to determine the RMS noise and the dynamic lag, use Matlab to calculate the root mean squared sum of the two parameters. In this case the optimum position estimation gain will be $\alpha = 0.29$ from the graph. Using the Benedict-Bordner relationship, the velocity estimation gain, $\beta = 0.049$.

For a 50Hz sample period, the filter bandwidth can be obtained from Figure 13.9 by interpolation and scaling to be about 3.5Hz

```

% determine the optimum tracking gains for an
% ablag.m
acc = 10;           % target acceleration
fs = 50;           % sample frequency
snrdb = 10;        % SNR
tau = 3;           % Range gate size(m)
snr = 10.^(snrdb/10);
ts = 1/fs;
% Calculate the RMS range tracking noise out of the split gate
% from the pulse width and the signal to noise ratio
sigma = tau/(2.5*sqrt(2*snr));
k=0
sigmaout=zeros(1,90);
alp=zeros(1,90);
lag=zeros(1,90);
for alpha=0.1:0.01:1,
    k=k+1;
    beta = alpha.^2/(2-alpha);
% position transfer function for the alpha beta filter
    b=(alpha, beta-alpha);
    a=[1,beta+alpha-2,1-alpha];
% measure the power in the impulse response to determine the VRR
    sig=zeros(1,500),ones(1),zeros(1,500)];
    out=filter(b,a,sig);
    alp(k)=alpha;
    vrr=sum(out.^2);
% calculate the noise after the track filter
    sigmaout(k) = sigma*sqrt(vrr);
% calculate the dynamic lag from the formula
    lag(k) = acc*ts.^2*(1-alpha)/beta;
end
comb = sqrt(lag.^2+sigmaout.^2);
plot(alp,lag,alp,sigmaout,alp,comb);
grid
xlabel('alpha')
ylabel('dynamic lag and RMS noise (m)')
title('Optimising the Filter Gain')

```

13.3.Range Tracking Systems

Most range tracking systems are associated with angle trackers to produce a full 3D tracking capability as discussed in Chapter 15. However, there are a number of applications in which the angular pointing function is either non existent or performed manually. Good examples of the latter are combined optical and ranging systems like close-in weapon systems or even some radar or lidar speed traps.

13.3.1. Lidar Speed Trap

As discussed in Chapter 7, laser range finders provide the most cost-effective method to measure long range in benign environments because very narrow beamwidth can be achieved using low cost optics.

This allows for high angular resolution measurements to be made.

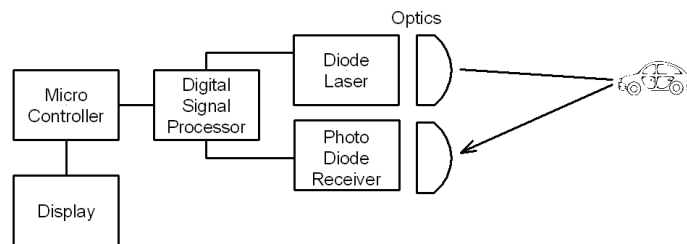


Figure 13.13: Laser radar operational principle

In the typical configuration shown in the figure above, the standard pulsed time of flight measurement technique is followed by a second micro-controller that processes the measured data to estimate the position and speed of the target.

Estimates the velocity can be made using a tracking filter of the kind discussed above, or by measuring the change in range as determined by the varying time of flight between successive pulses. From the figure below it can be seen that once the filter has settled, the estimates are smoother than those produced by the difference method. The amount of smoothing is determined by the value of the gains.

In practical applications, the filter is seeded with a reasonable estimate of the rate based on the position difference over a few samples. This speeds convergence considerably.

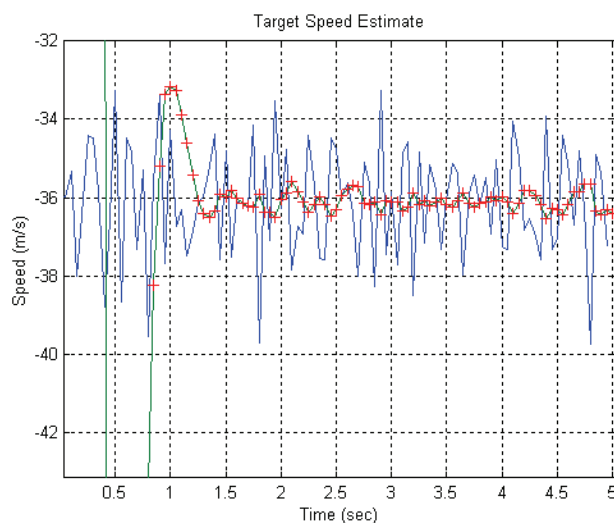


Figure 13.14: Tracker performance comparison between an $\alpha\beta$ filter estimate of the speed and a simple difference shows the superiority of filtering

```

% laser radar range tracking simulation
% uniform distribution of range error +/-10cm
% sample rate 20Hz
xtar = 400; % start range of target (m)
vtar = -130.0; % speed km/h
v = vtar/3.6; % speed m/s
fs = 20.0; % sample rate (Hz)
ts = 1/fs; % sample time (sec)
% determine the actual position of the car with time
t=(0:ts:5); % allowed time to get a fix 5s
x=xtar+v*t;
% uniformly distributed range errors between -0.1 and +0.1m
xnoise = 0.2*(rand(size(t))-0.5);
xmeas=x+xnoise;
% measure rate by subtracting pairs of pulses
rate=diff(xmeas)./ts;
len=length(rate);
t1=t(1:len);
%plot(t1,rate);
% measure the rate by filtering using an anpha beta filter
alpha = 0.5;
beta = alpha.^2/(2-alpha);
b1=(alpha,beta-alpha); % position transfer function
a1=(1,beta+alpha-2,1-alpha);
b2=beta*([1,-1,0])/ts;
a2=a1;
xdfil=filter(b2,a2,xmeas); % rate transfer function
plot(t1,rate,t,xdfil,t,xdfil,'+')
grid
title('Target Speed Estimate');
xlabel('Time (sec)');
ylabel('Speed (m/s)')

```

Riegl FG21-P



- Operating principle pulsed time of flight
- Beamwidth 2.5mrad
- Measuring time 0.4 to 1s
- Speed 0-250km/h
- Accuracy +/-3km/h to 100km/h
+/-3% of reading above 100km/h
- Range 30-1000m
- Accuracy +/-10cm typical
- Target marker, circular reticle
matched to beam diameter

Figure 13.15: Riegl speed scope



Figure 13.16: Effectiveness of narrow beam for measuring speed on congested roads

13.4. Angle Measurement

13.4.1. Amplitude Thresholding

At its most simple, a received echo amplitude threshold can be used to determine that a target is within the beam. This gives a very rough measure of the target direction.

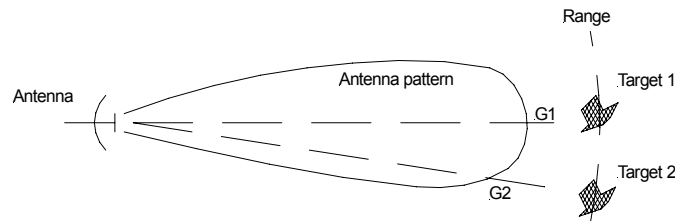


Figure 13.17: Antenna gain as a function of angle

Note that because the antenna gain drops off sharply, the angular position uncertainty is usually constrained to within the 10dB (one way) beamwidth of the antenna.

Both pulsed and CW techniques can be used for angle measurement over a broad range of frequencies from microwave to the infrared band. In general complex modulation schemes are generally used for the following reasons:

- Discriminate against ambient solar radiation,
- Eliminate interference from fluorescent lights,
- Reduce the probability of interference from other sensors.

One of the disadvantages of this technique is that the cross-range resolution degrades with range because sensors operate with a constant angular resolution, as shown in the figure below.



Figure 13.18: The cross range resolution degrades with range as shown. At position (a) the targets are resolved but at position (b) the targets, with the same spacing, are not resolved

The main applications are limited to CW or modulated IR proximity detectors for industrial & robotic applications.

Proximity Detector Example

IR proximity detectors are commonly used for short range robotic applications but not normally used to measure range, just the presence of a target within the beam. They operate in the near IR (at a wavelength just longer than visible light, typically 880nm) and are visible to CCD's so can be observed using a video camera (which can be useful)

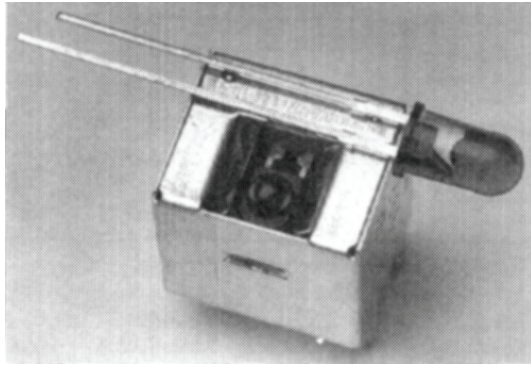


Figure 13.19: Infrared proximity detector

A typical receiver made by Sharp Electronics (GP1U52X) is shown here with a near infrared LED transmitter.

This receiver package includes a photodiode, amplifiers, filters and a limiter. The receiver responds to a burst modulated 40kHz signal with an on-off period of 600+600 μ s. The digital output goes low is a target is detected.

13.5. Angle Tracking Principles

13.5.1. Scanning Across the Target

Using the antenna beam pattern, it is possible to get a more accurate bearing on the target by sweeping the beam across it and noting changes in the signal amplitude. This process can increase the angular resolution with only a marginal effect on the range accuracy, however it relies on a good SNR for best results.

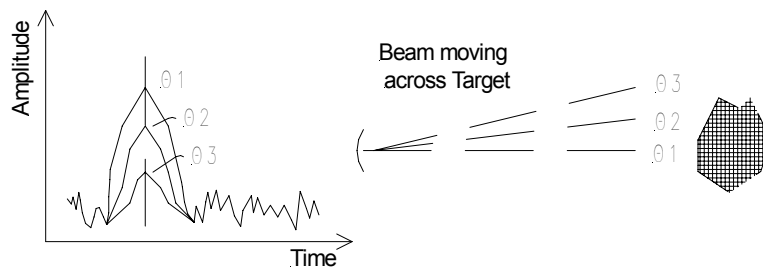


Figure 13.20: Using the beam pattern to estimate angle

13.5.2. Null Steering

Null steering involves the subtraction of the returns from a pair of overlapping beams to produce a “null” when the target is aligned with the beam axis of symmetry. Extremely accurate angle measurements can be achieved. For a point target, the theoretical improvement in angle measurement accuracy in thermal-noise is limited only by the signal to noise ratio of the measurement

$$\sigma_t = \frac{\theta_{3dB}}{k\sqrt{2(S/N)}} \text{ deg} \quad (13.12)$$

where: θ_{3dB} – Antenna Beamwidth (deg)
 k – Constant dependant on the tracking type
 S/N – Signal to noise ratio

The following are the most common null steering techniques:

- Lobe Switching
- Conical Scan
- Monopulse

13.6.Lobe Switching (Sequential Lobing)

This technique involves sequential transmission from two antennas with overlapping but offset beam patterns.

Sequential returns will be amplitude modulated if the target is not on boresight. This AM can be used to generate an angle error estimate, or used to drive the antenna to null the error.

Two additional switching positions are needed to obtain the angular error in the orthogonal axis, so 4 pulses are required to control the antenna in 2D.

This technique can be used for EM or acoustic tracking systems and most non scanning collision avoidance radars use this technique with either 2 or 3 lobes to determine the angular offset of cars. In addition a passive version of lobe switching is often used for direction finding applications as discussed in the example at the end of this chapter.

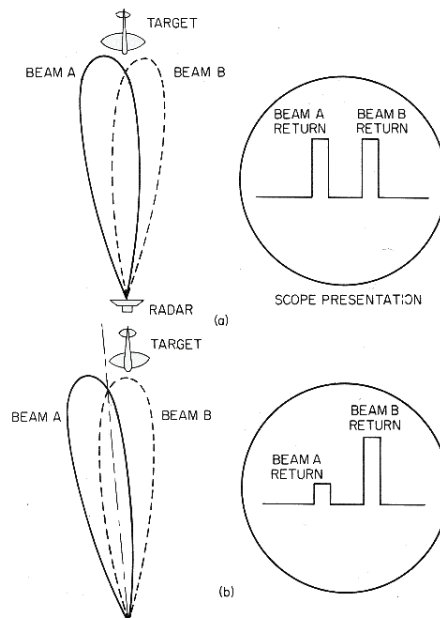


Figure 13.21: Principle of sequential lobbing to determine angle error

13.6.1. Main Disadvantages of Lobe Switching

This technique results in a reduced bandwidth because 4 pulses are required to resolve the target in 2D.

Fluctuations in the signal level due to variations in the echo strength on a pulse-by-pulse basis reduce the tracking accuracy so it is susceptible to modulation by the target, either natural (propellers, wing beats etc.) or as part of the electronic countermeasures.

The antenna gain in the on boresight direction is less than the peak gain, so the peak gain is reduced with a consequent reduction in the maximum operational range.

13.7. Conical Scan

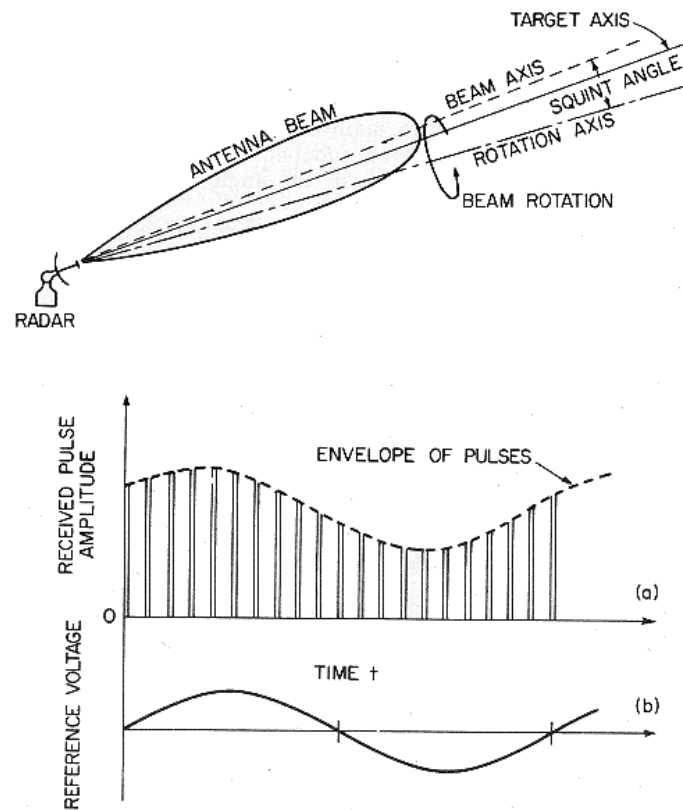


Figure 13.22: Principle of conical scanning to determine angle error

A single beam displaced in angle by less than the antenna beamwidth is nutated on its axis. (Nutated means spinning without rotating the polarisation). Beam displacement is often achieved by incorporating a rotating sub-reflector in a Cassegrain antenna as shown in the figure below.

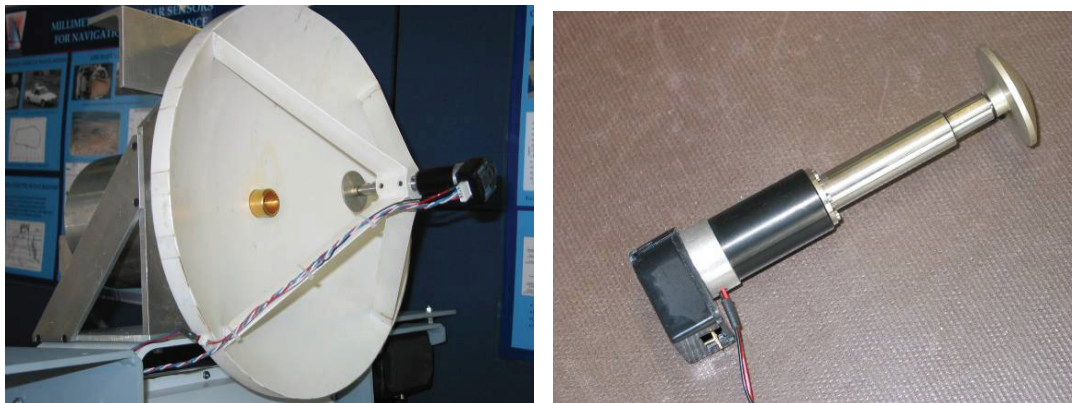


Figure 13.23: Cassegrain antenna with a canted spinning sub-reflector to implement conical scan

The scan rate is generally limited to between 5 and 25 pulses per revolution for long range operation, but at short range where the PRF is higher, many more pulses are

received. Amplitude modulation of target returns will be a function of the position of the boresight with respect to the target and phase detectors (multipliers) using quadrature phase references for the two orthogonal axes demodulate the received AM signal out of the range tracking gate to generate the angle tracking error as described in the following section.

There are a number of different methods that can be used to perform this demodulation function as shown in the following figure.

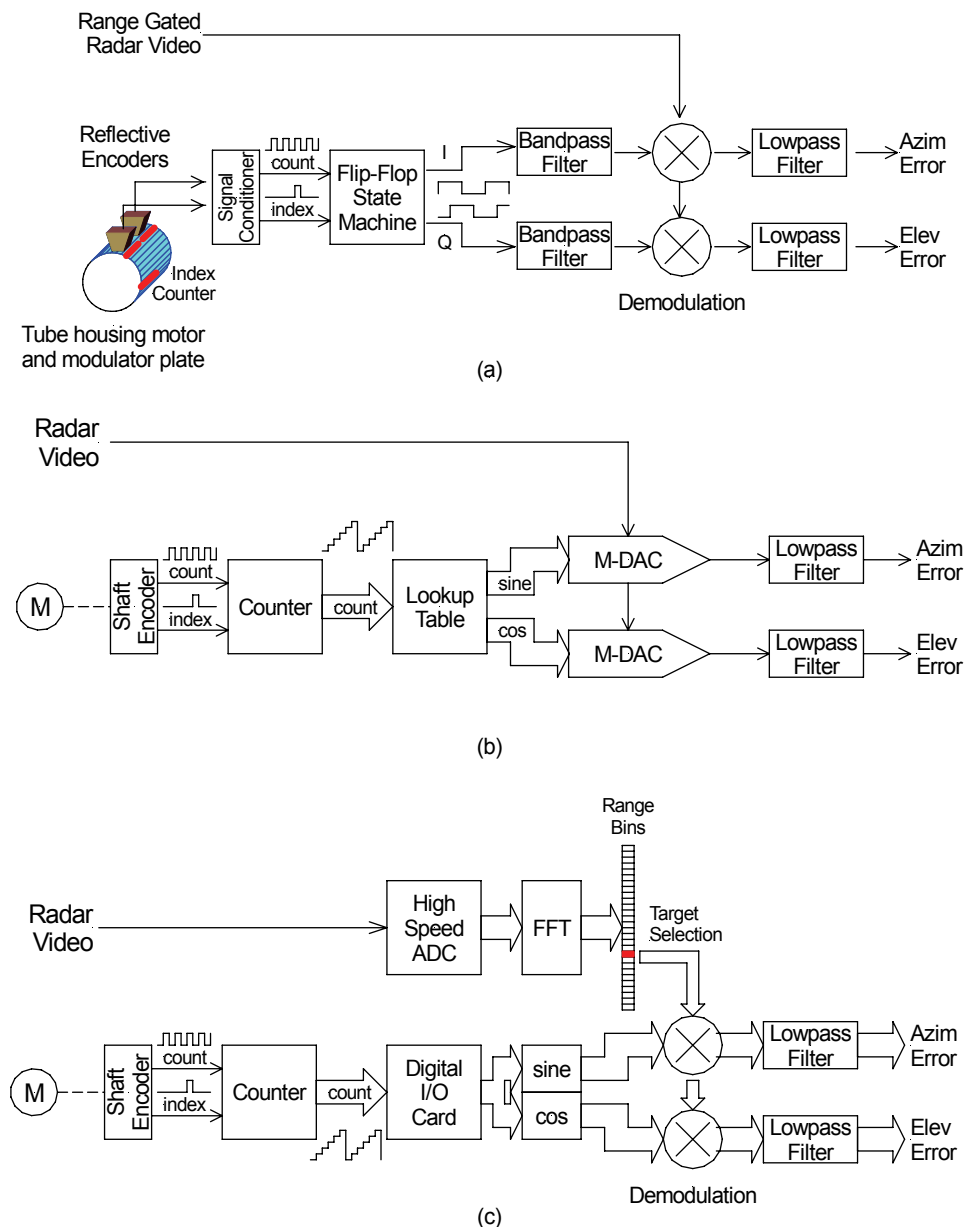
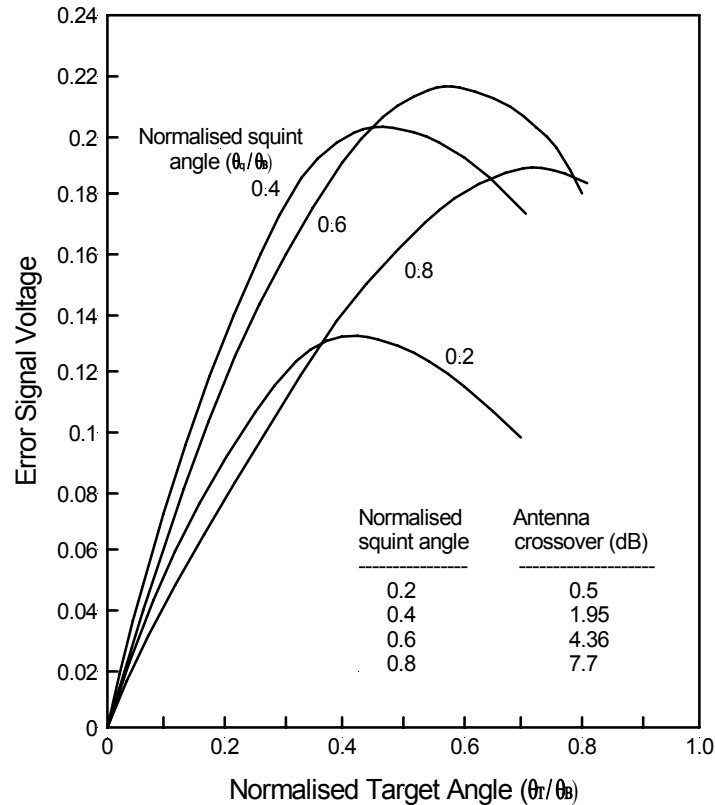


Figure 13.24: Some conscan angle error demodulation techniques (a) analog, (b) digital in hardware and (c) digital in software

An implementation of the digital solution in software is discussed in detail in the following section.

13.7.1. The Squint Angle Optimisation Process

It can be seen in the figure below that the error voltage is a function of the squint angle and the target angular error each as a function of the antenna beamwidth.



θ_q – Squint angle θ_T – Target angle θ_B – Antenna 3dB beamwidth

Figure 13.25: Error voltage as a function of target angle with squint angle as a parameter

The greater the slope of the error signal, the more accurate will be the angle tracking. This occurs at θ_q/θ_B just greater than 0.4

The gain on boresight is about 2dB down on the peak

The range tracking accuracy is determined by S/N, and so requires the maximum on boresight gain $\theta_q/\theta_B = 0$ which is not feasible.

A compromise is used with $\theta_q/\theta_B = 0.28$, which corresponds to an antenna gain about 1dB below the peak.

13.7.2. The Transfer Function of a Conically Scanned Antenna

In the same way that a split gate range tracker can be characterised by its range transfer function, so too can an angle tracking system be characterised by its angle error transfer function.

To perform this measurement, a conscan antenna mounted on a pan-tilt unit, as illustrated in the following figure, is swept past a point source of radiation (in the far field of the antenna). The received signal level at the output of the antenna is logged as a function of angle (or time if the angular rate is constant).

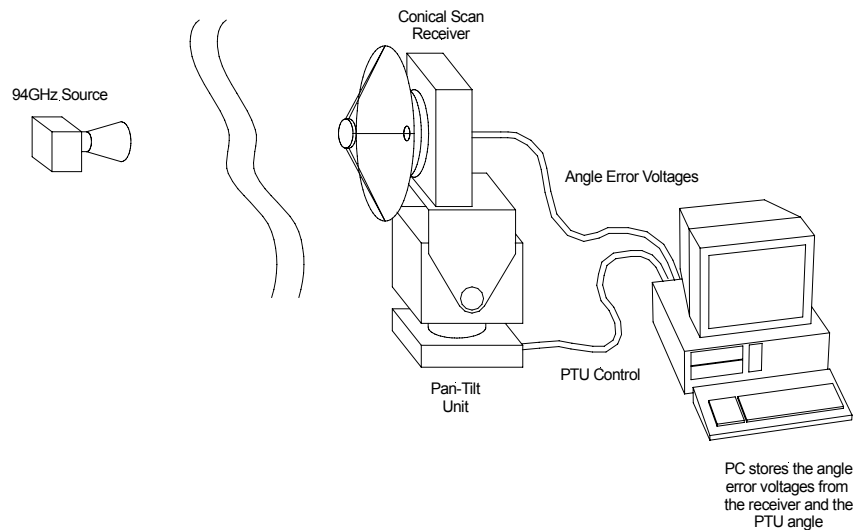


Figure 13.26: Mechanism for measuring conscan error transfer function

The received signal are as shown in the figure (a) below:

- The AC component of the signal level starts out low, when the offset is large
- It then increases to a peak when the beam squint angle equals the target offset on the one side
- On axis, the beam offset is symmetrical so there is no modulation, and so the AC component reduces to zero
- At the cross-over point the phase of the modulation is reversed but the shape of the modulation is the mirror image due to the symmetry of the process

In (b), both the modulation signal and the reference signal are shown. Note the 180° phase shift at crossover which is an indication that the sign of the error is reversed.

In (c), the synchronously demodulated signal is shown. Note that there is a DC component and an AC component at twice the modulation frequency.

Figure (d) shows the filtered demodulated signal showing only the DC which is the conscan angular transfer function for the Cassegrain antenna shown.

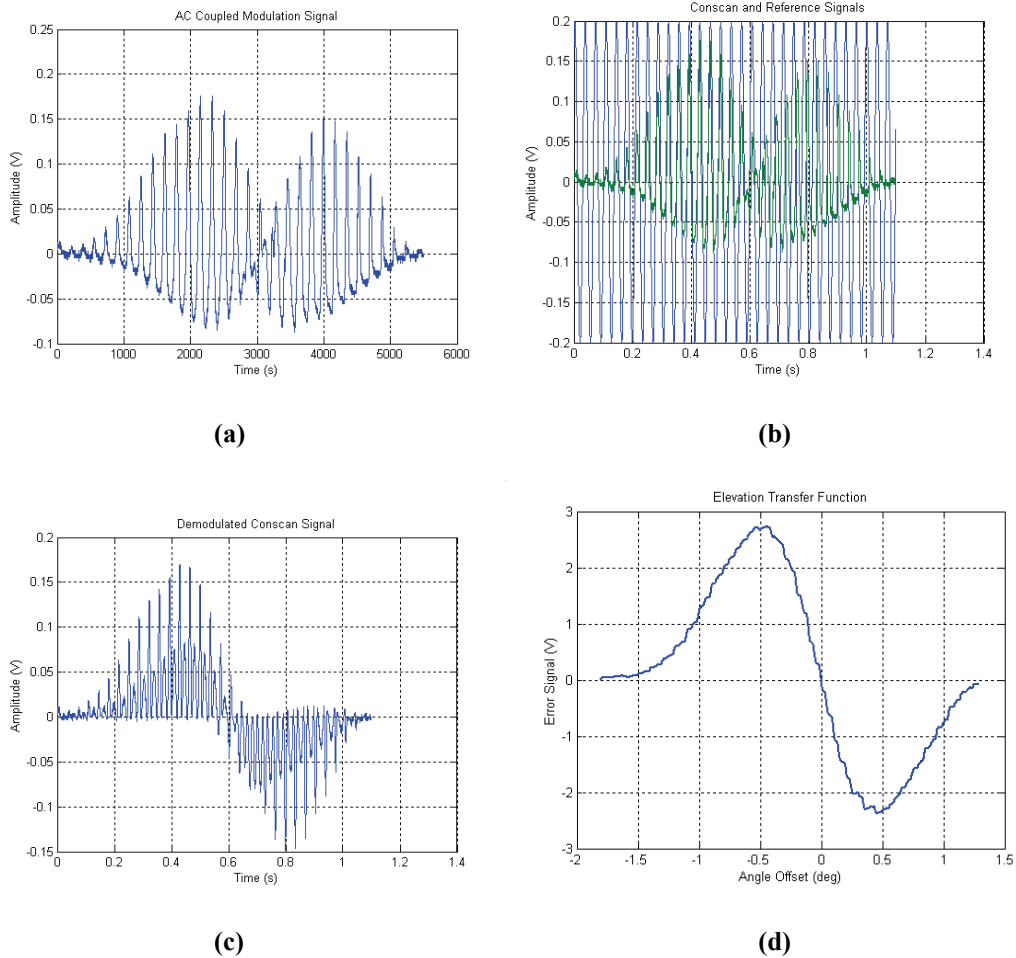


Figure 13.27: Conscon demodulation process showing the following: (a) modulated signal as antenna sweeps past source (b) modulated signal and reference signal showing phase reversal (c) the demodulation product of the signal and the reference (d) filtered demodulated error signal mapped to angle

13.7.3. Application

Conscan systems are typically used in tracking radars as shown in the figure below. They are simple to implement, using a single beam and a single receiver and transmitter, and beacon tracking can be implemented without the transmitter and without the range gating circuitry.



Figure 13.28: Conscon radar tracker on pedestal

As shown in the schematic diagram of the tracker, below, the AM signal out of the range gate is demodulated by the azimuth and elevation reference signals to produce the two angle error signals.

These angle errors drive the angle servos which in turn control the position of the antenna, and drive it to minimise the error (a null tracker).

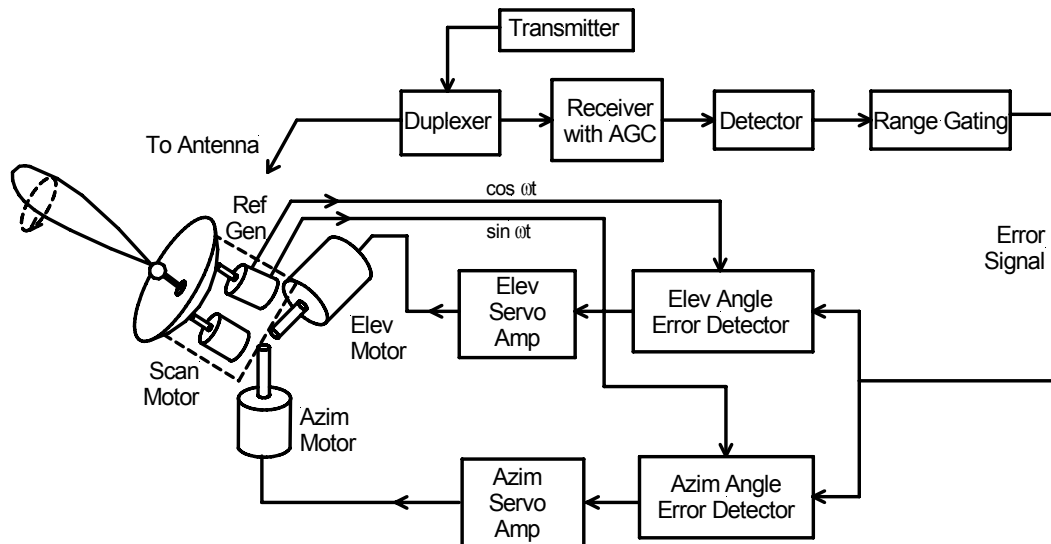


Figure 13.29: Block diagram of a conical scan radar

13.7.4. Main Disadvantages

The tracking bandwidth is reduced because of the number of pulses required to produce each error estimate.

Fluctuations in the echo signal amplitude induce tracking errors and so these systems are sensitive to target modulation. However modified conscan techniques have been developed to eliminate the modulation problem:

- Dual Conscan (Russian Design)
- COSRO (Conscan on receive only)

The antenna gain is reduced on boresight due to the squint angle. A trade-off is required to optimise the tracking accuracy.

13.7.5. Other considerations

Automatic Gain Control (AGC) that is required to normalise the pulse amplitude for range tracking must be carefully designed not to interfere with the conscan modulation.

13.8. Amplitude Comparison Monopulse

In essence this technique uses two overlapping antenna beams for each of the two orthogonal axes that are generated from a single reflector illuminated by 4 adjacent feed horns. The difference in the amplitude (or phase) of the signals output by these beams is used to derive the angle errors in both elevation and azimuth.

13.8.1. Antenna Patterns

The sum pattern, Σ , of the 4 horns shown in the figure below is used on transmit and for range measurement on receive.

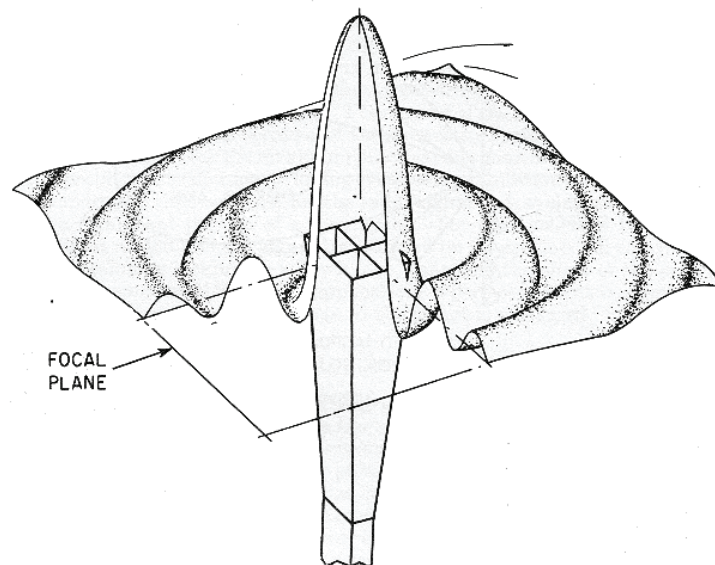


Figure 13.30: Monopulse sum-channel beam pattern

On receive the four horns produce 3D beam patterns as shown in the figure below.

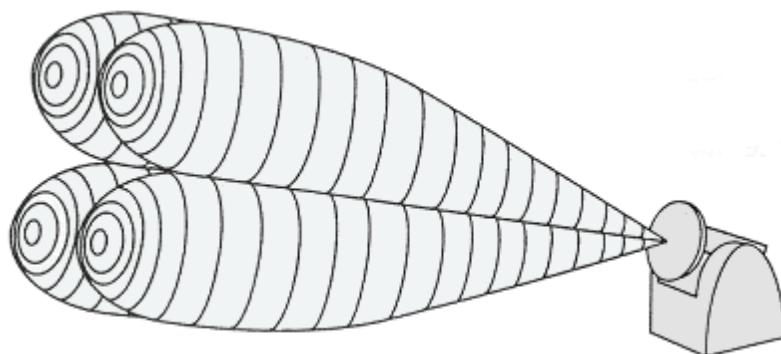


Figure 13.31: Monopulse difference-channel beam patterns

When viewed from the front, the beam patterns are as shown in the cross section shown below.

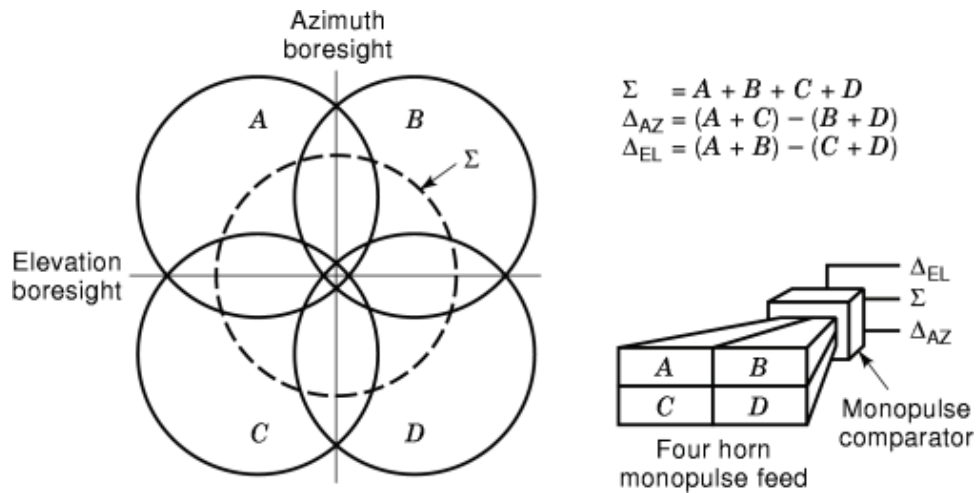


Figure 13.32: Combining beams using a microwave hybrid circuit (monopulse comparator) to produce sum and difference channel signals

13.8.2. Generation of Error Signals

The difference patterns Δ_{AZ} and Δ_{EL} are produced on receive using a microwave hybrid circuit called a monopulse comparator. The hybrids perform phasor additions and subtractions of the RF signals to produce output signals shown in the following figure.

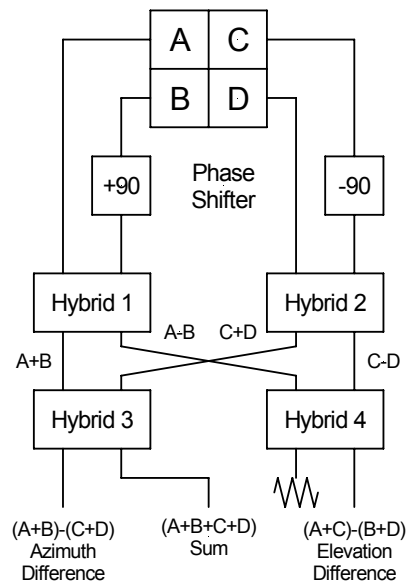


Figure 13.33: Hybrid configuration to produce sum and difference channel signals at the transmit frequency

It can be seen that if a target is on boresight, then the amplitudes of the signals received in the four channels (A,B,C,D) will be equal, and so the difference signals will be zero. However, as the target moves off boresight, the amplitude of the signals received will differ, and the difference signal will take on the sign and magnitude proportional to the error.

The difference channel signals are normalised with respect to the sum channel to produce an error signal that is independent of the echo amplitude as shown in the figure below.

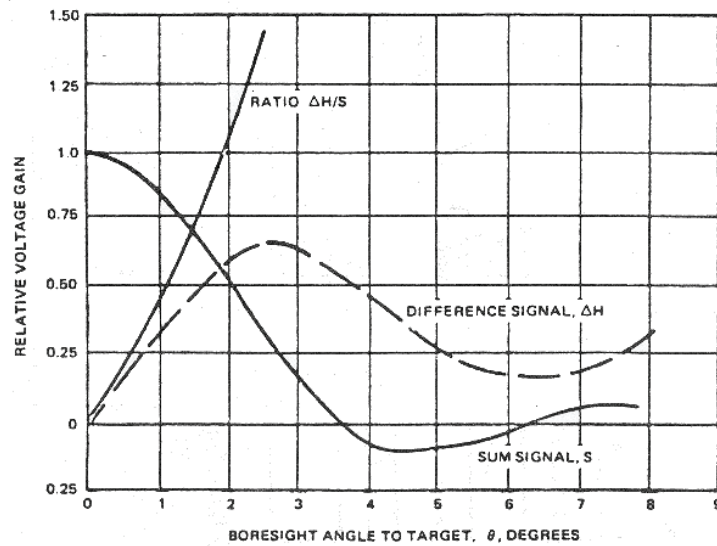


Figure 13.34: Normalised sum and difference channel gains as a function of angle off boresight

This ratio can be obtained using an AGC circuit that operates on the two difference channels and is driven by the detected sum-channel output of the tracking gate, or by division in a digital tracker.

Phase detectors demodulate the azimuth and elevation error signals using the sum channel IF signal as a reference to produce the two error voltages. These must also be range-gated so that their magnitudes represent the error signals from the correct target.

The sum and difference channel voltage signals can be modelled quite accurately using the following

$$\begin{aligned} E_{sum} &= \cos^2(1.14\Delta) \\ E_{dif} &= 0.707 \sin(2.28\Delta) \end{aligned} \quad (13.13)$$

where E_{sum} – Normalised sum channel output voltage,
 E_{dif} – Difference channel output voltage (normalised to sum channel),
 Δ - Angle from the beam axis normalised wrt to the half power sum channel beamwidth.

New error measurements are produced with every pulse, hence MONOPULSE

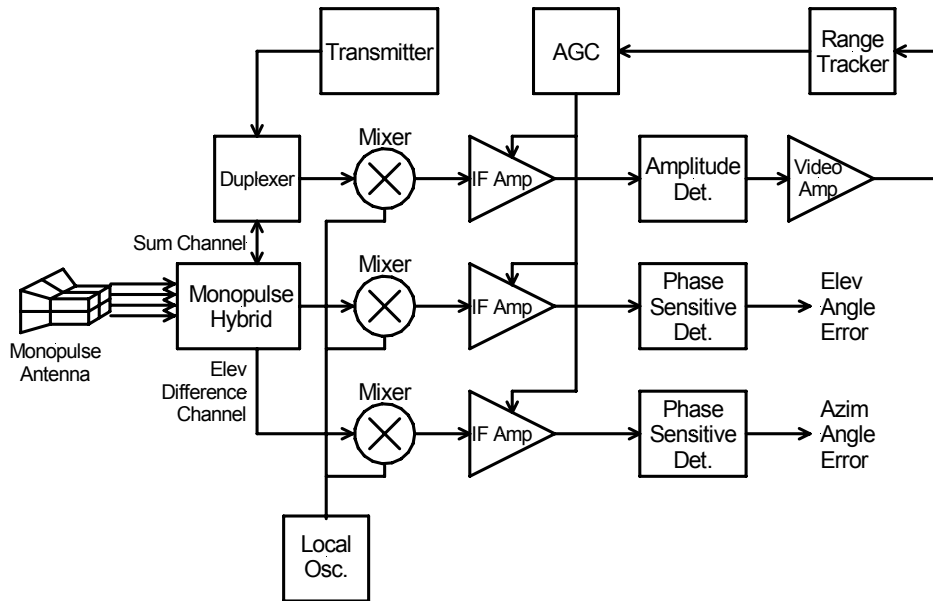


Figure 13.35: Schematic diagram of a monopulse front end

13.9. Comparison between Conscan and Monopulse

The monopulse option gives greater SNR for the same size target due to the higher on-boresight antenna gain, only the gains of the difference channel signals are reduced by the beam squint angle. In addition the steeper error slope near the origin results in superior tracking accuracy, and because new tracking information is generated with each new pulse, tracking is not degraded by fluctuations in echo amplitude.

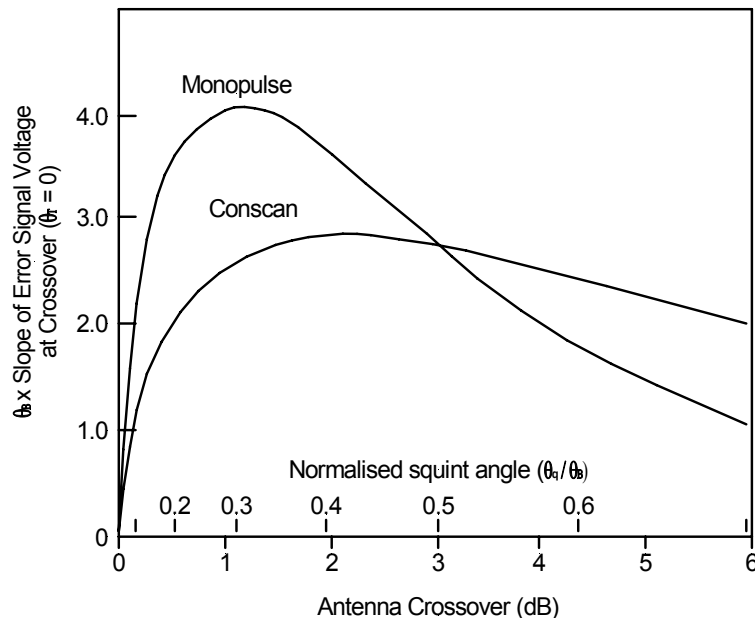


Figure 13.36: Error signal slope as a function of squint angle

13.10. Angle Tracking Loops

Unlike the range tracking loop in which the gate position is controlled electronically, in an angle tracker the beam must be physically displaced in angle to minimise the azimuth and elevation tracking errors.

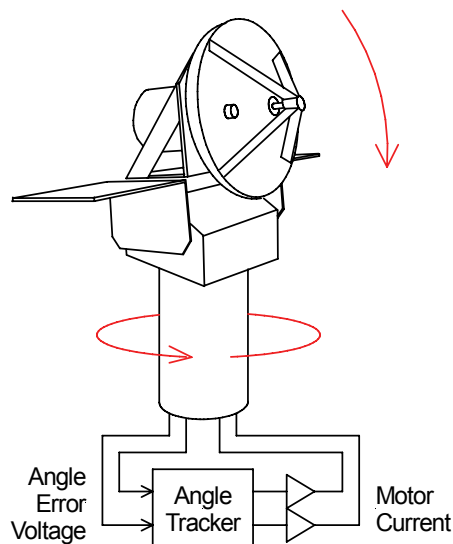


Figure 13.37: Angle tracking loop rotates the antenna to minimise tracking error

This physical displacement is achieved by supplying the angle servos with the error signals from the conscan or monopulse modules. These servos power the motors which rotate the antenna in the correct direction.

The RMS tracking error due to thermal noise is now

$$\sigma_t = \frac{\theta_{3dB}}{k\sqrt{2(S/N)f_r/\beta_n}} \text{ deg.} \quad (13.14)$$

where: θ_{3dB} – Antenna Beamwidth (deg),
 k – Constant dependant on the tracking type,
 S/N – Signal to noise ratio,
 f_r – Radar pulse repetition frequency (Hz),
 β_n – Angle servo bandwidth (Hz).

13.11. Angle Estimation and Tracking Applications

In combination with range trackers as shown in the schematic above, monopulse techniques are generally used for modern tracking radar systems. The technique can be used for direction finding (DF) systems or beacon tracking in passive receivers. The principle can be used by EM or acoustic systems, and quadrant detectors that apply the same basic principles are generally used by laser trackers to estimate angle errors.

13.11.1. Example of an Acoustic Tracker

Two receiver transducers are mounted with a slight outward squint so that if the acoustic signal from the beacon arrives at an angle, the signal amplitude received by one of the receivers will be higher than that received by the other. Only when the illumination is symmetrical will the two signals be equal as shown in the figure below.

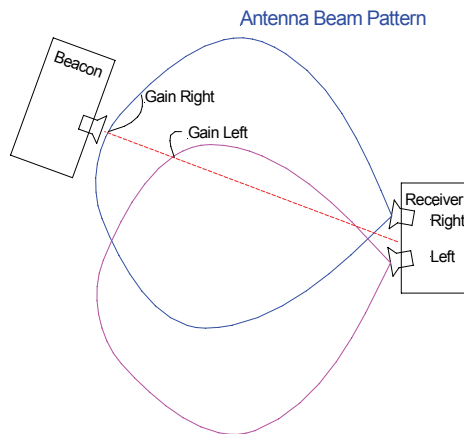


Figure 13.38: Conceptual diagram showing analog angle measurement

A simulation model was built using the ultrasonic transducer normalised gain pattern supplied by the manufacturer as shown in the polar plot below.

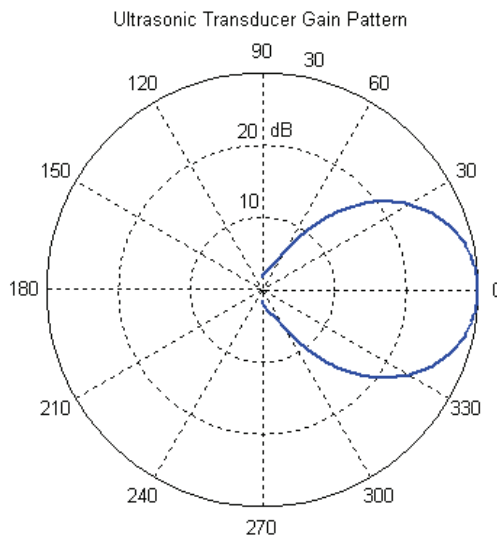


Figure 13.39: Polar pattern of ultrasound sensor normalised gain

The difference between the signal voltages received from the left and the right transducer is calculated to produce the receiver transfer function as shown in the following figure. It can be seen that the peak magnitude of the error signal is dependent on the squint angle. It can also be seen that there is a region of about $\pm 20^\circ$ over which the relationship between the voltage and the beacon angle is almost linear.

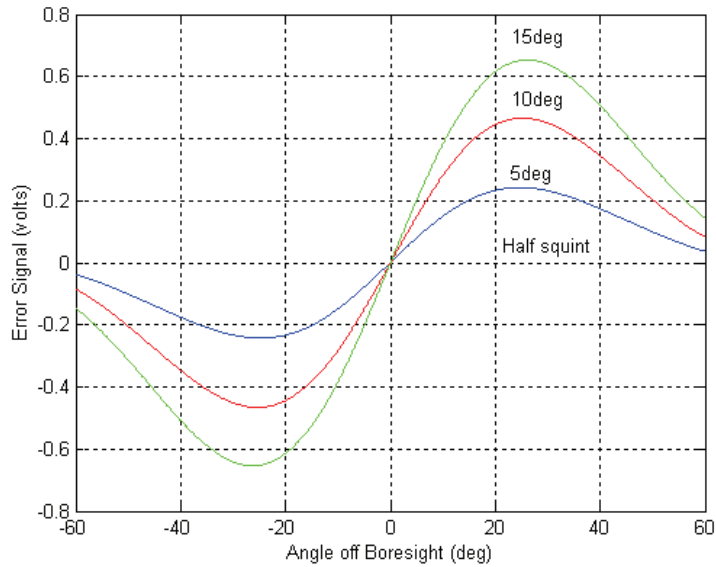


Figure 13.40: Angle error transfer function with squint angle as a parameter

13.11.2. Instrument Landing System (ILS)

An inverted application of the monopulse, dual beam concept

The ILS facilities are a highly accurate and dependable means of navigating an aircraft to the runway in low visibility

It consists of

- A localiser transmitter
- A glide path transmitter
- An outer marker (can be replaced by a non directional beacon or other fix)
- The approach lighting system

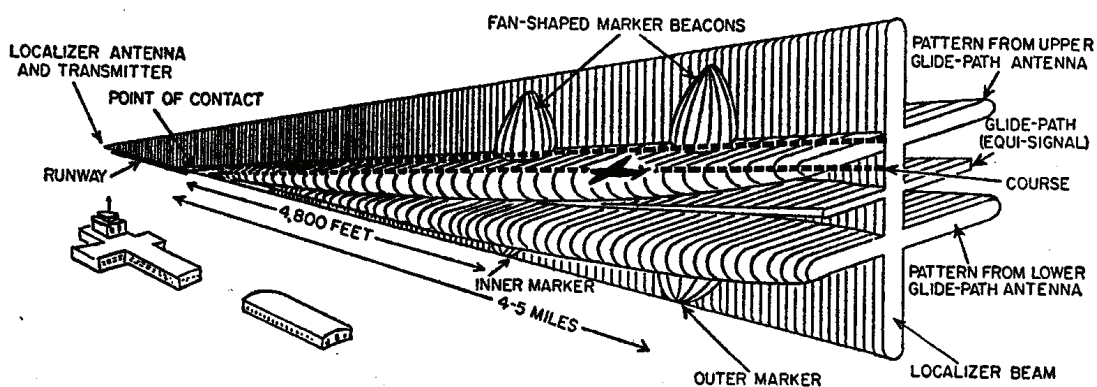


Figure 13.41: ILS signal patterns

A category I ILS provides guidance information down to a decision height (DH) of 200ft and with good equipment ILS can even be used for Category II approaches, 100ft on the radar altimeter. The ILS provides both lateral and vertical guidance necessary to fly a precision approach if glide slope information is provided.

Localiser Transmitter

The transmitter provides lateral guidance. It operates at VHF in the range 108.1MHz to 111.95MHz. The transmitter and antenna are situated on the centreline at the opposite end of the runway from the approach threshold. The antenna radiates two vertical fan shaped beams that overlap at the extended centre line of the runway. To differentiate between the two overlapping beams that are radiating at the same frequency, the right hand side of the beam (as seen by an approaching aircraft) is modulated at 150Hz and the left hand beam at 90Hz. The total width of the beam pair can be varied between 3° and 6°. It is adjusted to provide a track signal 700ft wide at the runway threshold increasing to 1nm wide at a range of 10nm.

Localiser Receiver

The localiser receiver activates the needle of one of the cockpit instruments as illustrated above. For an aircraft to the right of the beam, in the 150Hz region only, the needle will be deflected to the left, and visa versa in the 90Hz region. In the overlap region, both signals apply a deflection force to the needle causing a deflection in the direction of the strongest signal so that when the aircraft is precisely aligned, there will be zero net deflection, and the needle will point straight down..

Glide Slope Equipment

The glide slope equipment consists of a transmitter and antenna operating in the UHF at a frequency between 329.30MHz and 335.00MHz. It is situated between 750 and 1250 ft down the runway from the threshold, offset 400 to 600ft to the one side of the centreline and it is monitored to a tolerance of +/-0.5°. It consists of two overlapping horizontal fan beams modulated at 90 and 150Hz respectively and the thickness of the overlap is 1.4°, or 0.7° above and below the optimum glide slope. The glide slope may be adjusted between 2 and 4.5° above the horizontal plane depending on any obstructions along the approach path. Because of the antenna construction, no false signals can be obtained at angles below the selected glide slope, but are generated at multiples of the glide slope angle. The first is at about 6°. It can be identified because the instrument response is the reciprocal of the correct response.

The glide slope signal activates the glide slope needle in a manner analogous to that of the localiser. If there is sufficient signal, the needle will show full deflection until the aircraft reaches the point of signal overlap, at this time the needle will show partial deflection in the direction of the strongest signal. When both signals are equal, the needle shows horizontally indicating that the aircraft is precisely on the glide path. With 1.4° of overlap, the glide slope area is approximately 1500ft thick at 10nm reducing to less than 1ft at touchdown. A single instrument provides indication for both vertical and lateral guidance.

13.12. Triangulation

Though triangulation is not really a range or angle estimation technique, it is probably the most common method in use today for measuring the position of a target in space.

The basic technique is thousands of years old and includes the following options

- Bearing only
- Range only
- Hybrid range and bearing

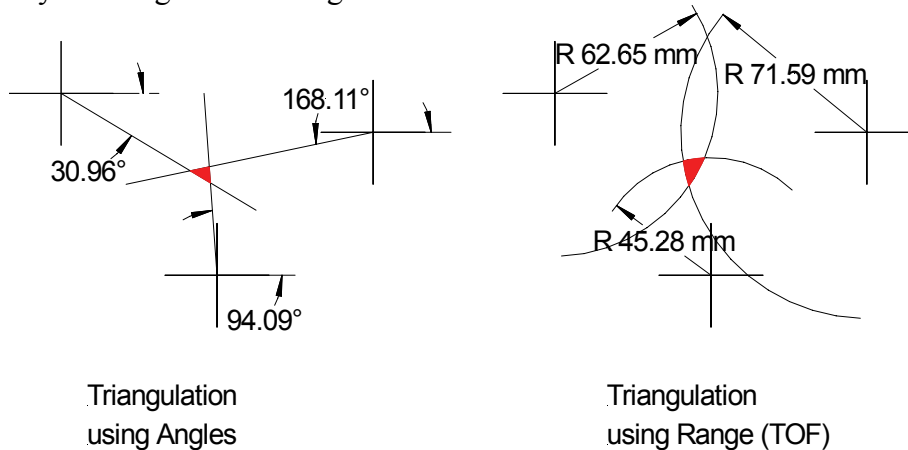


Figure 13.42: Position estimation by triangulation

Applications include

- Navigation: GPS, Omega, Loran-C
- Optical surveying
- Laser triangulation
- Radio emission detection
- Pinpointing earthquakes

13.12.1. Loran-C

LoRaN is an acronym for Long Range Navigation. It is a highly accurate (though not as accurate as GPS) highly available, all weather system for navigation in the coastal waters around the US and many other countries. An absolute accuracy of better than 0.25nm is specified within the region of coverage. And as with GPS, it is also used as a precise time reference,

A chain of three or more land based transmitting stations each separated by a couple of hundred km is used instead of a constellation of satellites. Within the chain, one station is designated as the master (M), and the other transmitters as secondary stations conventionally designated V,W,X,Y,Z.

The master station and the secondaries transmit radio pulses simultaneously at precise intervals and a Loran-C receiver on-board a ship or aircraft measures the slight difference in the time of arrival of the pulses. The difference in the time of arrival for a given master-secondary pair observed at a point in the coverage area is a measure of the difference in distance from the vessel to the two stations

The locus of points having the same TD from the pair, is a curved line of position (LOP). These curved lines are hyperbolas, or more correctly spheroidal hyperbolas on the curved surface of the earth and the intersection of two or more LOPs from different master-secondary pairs determines the position of the user as shown in the figure below.

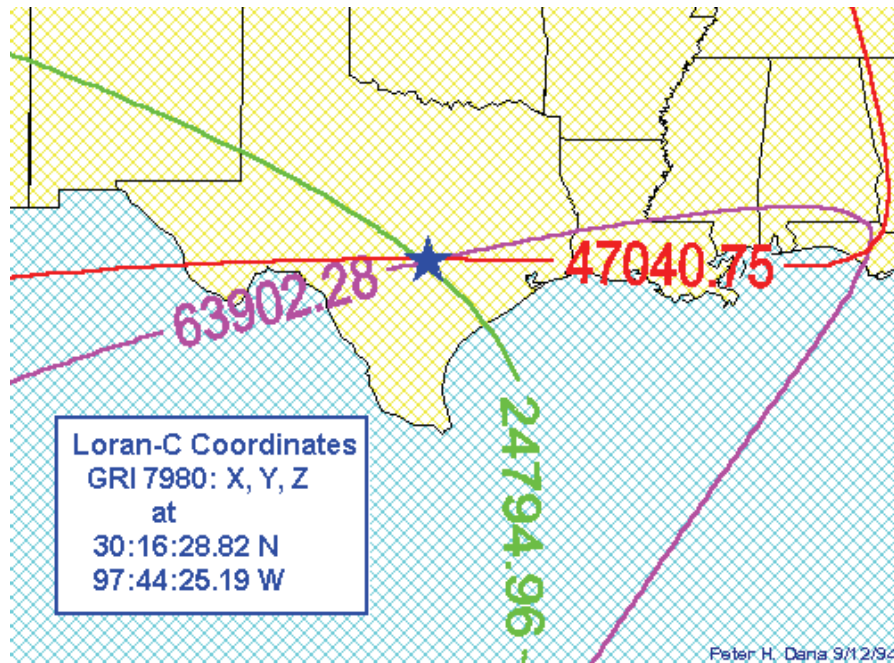


Figure 13.43: Intersection of two LOPs determines the receiver position

Why would anyone want Loran-C?

- it is inexpensive to operate, at \$17 million per year and user equipment is low-cost and of proven capabilities. GPS requires in excess of \$500 million per year.
- Loran's signal format has an integrity check built in, the GPS does not. Loran is easy to service ÷ just drive to the transmitting station, GPS replacement requires a new satellite launch schedule.
- On-air time for Loran-C is about 99.99%, GPS about 99.6% These features have convinced over 25,000 users to sign petitions to keep Loran-C online to its original date, 2015.
- Foreign nations have purchased new solid-state Loran-C transmitters to form new Loran-C chains in Europe, China, Japan and Russia. This land-based navigation system is viewed as a desirable, stable complement to the future GNSS of the world civilian community.
- And Loran is totally unclassified and is operated by host country authorities ÷ not the U.S. military.

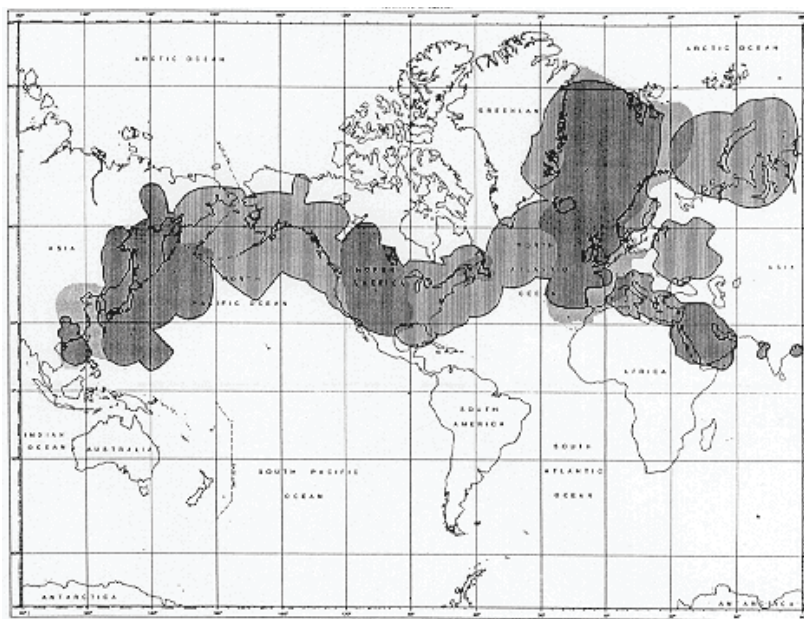


Figure 13.44: Loran-C coverage

Why does the military, who designed the GPS system, not rely on it totally?

- The ease of which GPS can be jammed either on purpose or by unexpected interferences is certainly a major reason. The deliberate jamming is well documented by the U.S. military, the International Association of Lighthouses and the Civil Aviation Authority (UK).
- A one watt jammer about 5x5x10cm with a 10cm antenna can block out a 60km diameter circle. Picture that near your local airport (such a unit costs about \$100.USD).
- If you want a jammer for GPS and Glonass, (the Russian equivalent to the GPS), such units were offered for sale by the Aviaconversia Company, Russia, which displayed them at a recent Moscow Air Show. Their jamming range was said to be 200km. What was the reaction by the FAA? "Nothing new" because there are "hundreds of these devices on the market".

13.13. References

- [1] D.Barton, *Radar Systems Analysis*, Artech 1976.
- [2] M.Skolnik, *Introduction to Radar Systems 2nd ed*, McGraw Hill, 1980
- [3] G.Morris, *Airborne Pulsed Doppler Radar*, Artech, 1988.
- [4] FG21-P –Principle of Operation, http://www.riegl.co.at/fg21p/21p_prin.html, 04/04/2000
- [5] SpeedTrap, http://www.audicoupe.demon.co.uk/speedtrap_types.html, 22/02/2000
- [6] M.Skolnik, *Radar Handbook*, McGraw Hill, 1970
- [7] N.Currie (ed), *Radar reflectivity Measurement: Techniques & Applications*, Artech House, 1989.
- [8] M.Skolnik, *Introduction to Radar Systems*, McGraw Hill, 1980
- [9] Navigation Systems- The Instrument Landing System, <http://www.allstar.fiu.edu/aero/ils.html>, 29/02/2000.
- [10] Marine Radio Beacons, <http://www.navcen.uscg.mil/policy/loran/h-book/book-1.txt>, 28/02/2000.
- [11] Loran C, http://www.landings.com/_landings/reviews-opinions/loran-c.html, 18/04/2001

